POLITECNICO DI TORINO
Repository ISTITUZIONALE

Effects of different cement-restorative material combinations in full-coverage onlay restorations: A FEA study

Original
Effects of different cement-restorative material combinations in full-coverage onlay restorations: A FEA study / Baldi, A., Scattina, A., Comba, A., Peroni, L., Rossi, T., Scotti, N.. - In: DENTAL MATERIALS. - ISSN 0109-5641. - ELETTRONICO. - 42:1(2026), pp. 78-90. [10.1016/j.dental.2025.09.011]

Availability:
This version is available at: 11583/3003615 since: 2026-01-04T12:49:23Z

Publisher:
Elsevier

Published
DOI:10.1016/j.dental.2025.09.011

Terms of use:

This article is made available under terms and conditions as specified in the corresponding bibliographic description in the repository

Publisher copyright
Elsevier postprint/Author's Accepted Manuscript

© 2026. This manuscript version is made available under the CC-BY-NC-ND 4.0 license http://creativecommons.org/licenses/by-nc-nd/4.0/.The final authenticated version is available online at: http://dx.doi.org/10.1016/j.dental.2025.09.011

(Article begins on next page)

28 November 2026

Effects of different cement-restorative material combinations in full-coverage onlay restorations: a FEA study.

1. INTRODUCTION

When cuspal coverage is needed [1], it has been demonstrated that indirect adhesive restorations (IAR) can efficiently restore severely compromised teeth while preserving tooth structure [2],[3],[4]. Residual dental tissue is a fundamental factor in the longevity of restorations, especially when dealing with endodontically treated teeth (ETT) [5],[6],[7]. Therefore, IAR have been encouraged and are nowadays showing promising clinical results [8],[9].

In order to match aesthetic and mechanical properties requests of clinicians, a variety of materials has been proposed for IAR. According to Gracis *et al.*, these materials comprehend milled resin composites, glass-matrix ceramics, polycrystalline ceramics and resin-matrix ceramics [10]. These materials present severe differences especially in mechanical properties, which are related to their specific composition [11]. A 2020 paper by Sulaiman *et al.* reviewed the essential mechanical properties of most materials used for IAR, reporting that milled resin composites have a flexural strength of 157-198MPa and an elasticity of 10.3-12.6GPa; hybrid materials, such as resin-matrix ceramics, have a flexural strength of 191-219MPa and an elasticity of 7.9-11.1GPa; glass-matrix ceramics have a flexural strength of 112.4.-420MPa and a modulus of elasticity of 48-95GPa; zirconia, the most common polycrystalline ceramic has a flexural strength of 557-1194MPa and an elastic modulus of 205-210GPa [12]. It is worth to highlight that this review, as well as similar papers, illustrate a great amount of data regarding the materials taken alone, but few information regarding their behavior when efficiently luted with different resin-based cements [13],[14]. For the present study, we selected for the simulation glass matrix-ceramic, polycrystalline ceramic and resin-matrix ceramic. These three groups are representative of most commonly used commercial materials for this type of restorations, but also possess important mechanical differences between each other.

Moreover, various protocols have been created for their cementation, combining adhesive systems, substrate pretreatments and cements [15]. Literature clearly showed how the performance of different adhesive systems depends on the substrate (dentin or enamel) and the surface pretreatment performed, with etched enamel performing the best [16],[17],[18]. However, there is still lack of data about the best approach in terms of which cement material perform the best. An ideal resin-based cement should be able to achieve good degree of conversion (DC) under the restoration, while maintaining low shrinkage stress and sufficient mechanical properties [19]. With these aims, two types of cements are today applied for the

cementation of adhesive restorations: dual-curing resin cements and light-curable composites. Dual-curing cements are commonly used because of their ability of being cured both trough light and chemicals, always leading to a proper DC [20]. On the other hand, light-curable composites present the best handling, but the DC is correlated to the light transmission through the restoration [20],[21]. Again, depending on the composition, these materials might present a wide range of shrinkage stresses and mechanical properties, that have been enlisted and evaluated in numerous papers [22],[23].

When simultaneously considering IAR materials and cements, the number of clinical scenarios increases, leaving no clear guidelines to the clinicians. Moreover, even if there are several mechanical tests available to efficiently evaluate the restoration-cement-tooth interface, anatomical variables make really hard to test all these combinations while maintaining a proper sample size. In this complex matter, Finite Element Method (FEM) has been introduced in dental research and proved useful to perform investigations of different materials in the exact same conditions, without prototyping [24]. This can help speeding up the procedure when lots of different material combinations need to be tested, simultaneously reducing biases related to the geometries of tested parts and biological samples quality. FEM has been validated by several studies as an effective research method for dental materials and is able to measure shrinkage forces and residual stresses of different restorative materials [25],[26],[27]. However, to the best of authors knowledge, few studies tested different combinations of cement-restorative materials and most of them used a conventional crown preparation design [28].

Given these considerations, the aim of the present study was to test, through FEM, different cement-material combinations in an IAR scenario generated through Micro-Computed Tomography (micro-CT). The null hypotheses tested were that there are no differences between tested (1) restorative materials and (2) cements.

2. MATERIALS AND METHODS

2.1 Specimen preparation

A single intact human lower first molar, extracted for periodontal reasons was selected and stored in distilled water after disinfection with an ultrasonic device. The study was granted ethics approval by the local ethics committee of the Dental School, University of XXX (DS-2018_No.001). The selected tooth was examined and confirmed to be sound, with no carious lesions, demineralization, cracks, or signs of wear under 20x magnification optical microscope. The sample was evaluated as representative of a common clinical scenario, both from an endodontic and restorative expert. No other samples were used, to avoid biases related to the

anatomical variability. Moreover, using multiple samples would complicate analyses without the benefit of comparing results between each other.

Pulp chamber opening was performed with a minimally invasive access and canals were shaped to the working length, set at the visible apical foramen (Pathfiles 1-3 and ProTaper Next X1-X3, Dentsply Maillefer, Ballaigues, Switzerland). The root canal system was not obturated with gutta-percha or cements, in order to avoid scattering artifacts in the micro-CT acquisition and considering that the focus of the study was the crown of the tooth rather than the radicular system.

A standard MOD cavity was then drilled on the specimen by an expert operator (+10 years of practice in restorative dentistry) to simulate a damaged tooth. Interproximal boxes were created with an extension of 4 mm in the buccal–oral direction and 2 mm in the mesio-distal direction, with the cervical margin positioned 1.5mm above the CEJ. As concerns the occlusal area, the cavity was performed setting residual wall thickness of buccal and oral cusps at the height of the contour to 2 ± 0.2 mm, measured with conventional caliper. For cavity preparation, cylindrical diamond burs (model 835KR; Komet, Schaumburg, IL, USA) under copious air-water cooling were used in a high-speed headpiece (Kavo Dental GmbH, Biberach, Germany). All internal edges were then smoothed and rounded with an Arkansas point (FG 645, Komet, Schaumburg, IL, USA), in order to remove non-sustained enamel and to create a continuity between the MOD cavity and the endodontic access.

A conventional build-up procedure was then performed as follow: selective enamel etching for 30 s with 35% phosphoric acid (K-etchant, Kuraray Noritake Dental, Mie, Japan), rinsing for 30 s, and air-drying. A two-step self-etch adhesive system (Clearfil SE Bond2; Kuraray Noritake Dental, Mie, Japan) was then applied following the manufacturer's instructions, and slightly air-dried before light-curing for 40 s with a light-emitting diode (LED) lamp at 1400 mW/cm^2 (Cefalux2; Voco, Cuxhaven, Germany). Then, 2 mm nanohybrid composite layers were applied progressively up to the occlusal surface (Clearfil Majesty ES-2, Kuraray Noritake, Mie, Japan), each being light-cured with the same LED lamp for 20 s.

After that, a beveled overlay preparation was performed, in order to obtain a uniform 1.5mm space for the restoration in the occlusal surface. In order to standardize restoration thickness, an initial anatomical reduction was performed with 1.4mm diameter cylindric bur (model 835KR; Komet, Schaumburg, IL, USA). Mesial and distal boxes were prepared with dedicated sonic points (n°34 and n°35, SonicFlex, Kawo, Shangai, China), cervically exposing enamel. Occlusal sharp edges were beveled with a football-shaped bur angulated at 45° (model 8379-021, Komet, Schaumburg, IL, USA). Finishing was performed with same-shape burs with

fine and extra-fine grit, then Arkansas (FG 645, Komet, Schaumburg, IL, USA) and rubber points.

Specimen was then scanned with an intraoral camera (Cerec Omnicam AC, Dentisply, Sirona, Konstanz, Germany) and an overlay was designed with a CAD system (Cerec 4.5.2 software, Dentisply, Sirona, Konstanz, Germany). Restoration was milled with a reinforced lithium silicate material, optimal for further segmentation in micro-CT (Celtra DUO, Dentsply, Sirona, Konstanz, Germany) in extra-fine mode (Cerec MC XL, Dentsply, Sirona, Konstanz, Germany). The parameter for luting space was set to 80 µm in the internal area and 10 µm in the 1mm-wide marginal area. Once milled, the restoration was crystallized following manufacturer instructions and a dedicated patented program (Cerec Speedfire, Dentisply, Sirona, Konstanz, Germany).

Cementation was carried out with a dual-cure resin cement suitable for greyscale segmentation (Panavia V5, Kuraray Noritake Dental, Mie, Japan) following manufacturer instructions. Excesses of cement were removed with a micro-brush, then, after three minutes of setting, photopolymerization was carried out for a total of three minutes (approximately 40 seconds per surface) with a LED lamp at 1000mW/cm2 (Celalux 2, Voco). Finishing and polishing were performed with fine and extra-fine diamond burs and rubber points on a handpiece. Margins were double-checked to exclude the presence of under-contours or over-contours, then the sample was confirmed to be clinically acceptable by an expert operator (more than 10 years of experience in prosthodontic field).

2.2 Micro-CT reconstruction

A Micro-CT scan (SkyScan 1172; Bruker, Billerica, MA, USA) was employed to recreate an accurate digital model of the tooth-restoration complex. The scan was performed using the following parameters: voltage = 100 kV; current = 100 µA; aluminum and copper (Al+Cu) filter; pixel size = 10 µm. NRecon software (Bruker, Billerica, MA, USA) was used to reconstruct the images and obtain DCM files (DICOM, Digital Imaging and Communications in Medicine) applying the following corrections: beam hardening = 30%, smoothing = 2, ring artifact correction = 9.

The obtained files were imported into a segmentation software (Mimics Medical ver. 20.0; Materialise, Ann Arbor, MI, USA). Thanks to the different radiodensity among materials, using the thresholding function, it was possible to create masks representative of enamel, dentin, restorative material, cement and build up. To manage artifacts, region growth was used to remove noise voxels, while the close function was applied to remove gaps. The contact was ensured using morphology and Boolean operations, expanding the masks and using subtraction

to avoid gaps and compenetrating parts in this phase. The final masks were then converted into optimal-quality STL files (STereo Lithography interface format), with a sample ratio 1:1.

2.3 Finite Element (FE) model preparation

The obtained STL files were imported into Meshlab (ISTI, CNR, Pisa, Italy) in order to perform the refinement and quality analysis of elements. This process consisted in the reduction in the number of elements and in the elimination of the degenerated elements, while simultaneously filling holes and fixing orientation. Commonly used quality parameters, such as aspect ratio, were used to evaluate the overall quality of the mesh.

The two-dimensional mesh was then converted into a tetrahedral mesh model using Altair Hyperworks (Altair Engineering, Troy, Michigan, USA). The obtained FE model has a total number of nodes equal to 23039. The number of nodes of each different part is reported in Table 1.

PART	**N° Nodes**
Chewing sphere	7351
Restoration	5127
Cement	6967
Enamel	8646
Build-up	2244
Dentin	7042

Table 1. Number of nodes of each part of the FE model.

Intermediate analyses were carried out to optimize the contact in between the surfaces, verifying and removing compenetrating parts that might lead to unwanted results.

Moreover, similarly to other FEM studies, a 6 mm diameter sphere was discretized using shell elements to apply to load with a tripod contact, while the tooth was restrained in the radicular aspect 2 mm below the CEJ to simulate bone level [29],[30]. This type of contact is commonly found in-vivo (with the mesio-palatal cusp of the first upper molar) and is also used to position the sample in chewing simulator tests. Figure 1 shows a representative picture of the obtained model.

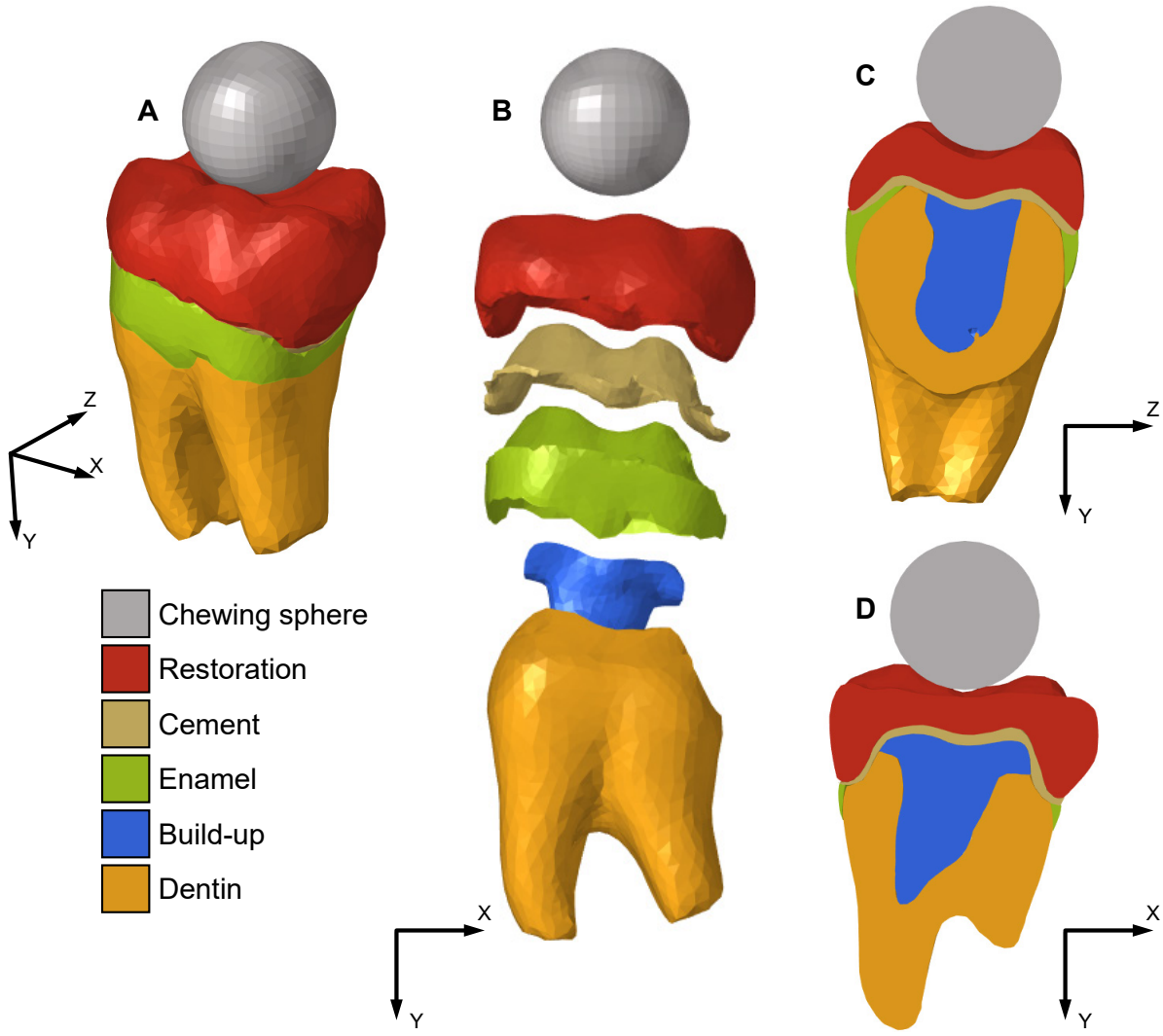


Figure 1. (A). Obtained Finite Element (FE) model; (B)Exploded view of the FE model; (C-D) cross sections of the FE model.

Periodontal ligament was not simulated, due to debates in literature regarding the best way to model it. Moreover, there is a consistent difficulty in measuring numerically the mechanical properties of the ligament itself, which might lead to additional biases. Finally, the study is focused on coronal structure, thus root boundaries were simplified to avoid displacement of the tooth-restoration system.

Three different restorative materials and two different resin cements were evaluated in the present study. This was meant to test the main categories of dental materials applied for IAR, for a total of six combinations, as follow:

Model A: Glass matrix ceramic (lithium disilicate) + Dual-curing resin cement

Model B: Glass matrix ceramic (lithium disilicate) + Light-curable composite

Model C: Polycrystalline ceramic (zirconia) + Dual-curing resin cement

Model D: Polycrystalline ceramic (zirconia) + Light-curable composite

Model E: Resin-matrix ceramic (reinforced resin composite) + Dual-curing resin cement

Model F: Resin-matrix ceramic (reinforced resin composite) + Light-curable composite

Table 2 reports a summary of material properties that were attributed to the single volumes, according to previous paper and manufacturers [29]. The dual-curing resin cement and the light-curable composite were purposely selected with similar Young's modulus but different volumetric shrinkage, in order to emphasize the effect of polymerization shrinkage stress on the models.

Material	**Young's modulus (GPa)**	**Poisson ratio**	**Density (g/cm^3)**	**Volumetric Shrinkage (%)**
Enamel	80	0.33	2.9	
Dentin	18	0.23	2.2	
Nanohybrid composite of build-up*	12.7	0.35	1.9	1.9*
Allumina sphere	80	0.23	2.7	
Glass matrix ceramic (lithium disilicate)	95	0.23	2.5	
Polycrystalline ceramic (zirconia)	210	0.3	6.03	
Resin-matrix ceramic (reinforced resin composite)	7.9	0.37	1.94	
Dual-curing resin cement *	8.3	0.24	2.23	5*
Light-curable composite *	6.7	0.33	1.85	1.9*

Table 2. Material properties of the FE parts, obtained from literature or provided from the manufacturers (*).

Dentin, enamel and restorative materials were modelled as linear and elastic, whereas the chewing sphere was modelled as a rigid material, because the deformation of this part is negligible compared to the others of the model. Sphere-tooth contact was created with an automatic surface-to-surface contact algorithm, positioning the sphere centered in the central fossa.

The FE simulation was performed using LS-Dyna code in its explicit and implicit formulations, also taking into account the residual stresses caused by polymerization shrinkage of resin-based materials, both of the build-up and the two tested cements. In order to do that, an initial implicit analysis was carried out, taking advantage of thermal variation to simulate

volumetric contraction of aforementioned materials. After this step, it was observed (Figure 2) that residual stresses are present both in the restoration-cement interface and in the cement-tooth interface. The Von Mises stress analysis on these are shown a quite regular distribution of stresses without significative presence of localized high stress area. In particular, the volumetric contraction is more regular and creates lower residual stresses using reinforced resin composite. With this condition considered as baseline, loading was applied through the sphere at the whole structure. This second simulation was set-up considering the explicit method. In order to avoid instabilities of the simulation, a motion law was applied to the sphere, with a constant 2 mm/s speed in the vertical direction up to the target load of 50 N. The contact between the sphere and the tooth was set as a penalty-based formulation, whereas the joining between the other parts (enamel, dentin and restorations) were defined with a tied contact formulation with offset option (Ansys LS-Dyna User Manual R16@e545952c7), to simulate proper interfaces. This type of contact is a constrained based contact, which creates a kinematic constraint between the two surfaces in contact, without affecting the original position of nodes, therefore without affecting the interface geometries.

Normal pressure and shear stress at the tooth-cement and the cement-restoration interfaces were recorded and are reported in the result section.

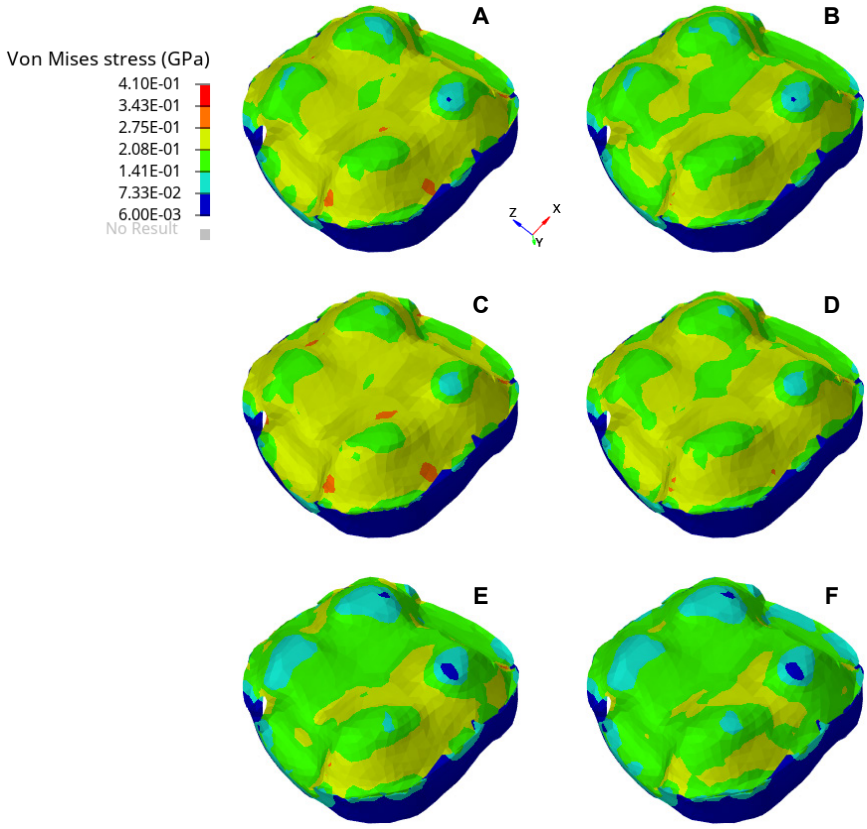


Figure 2. Resulting Von Mises stresses of the six tested models due to the polymerization shrinkage

3. RESULTS

3.1 Tooth-cement interface

Figure 3 reports the stresses along the three main directions on the tooth-cement interface. Regarding restorative material variable, resin-matrix ceramic models (E and F) were subjected to the highest stresses, followed by glass-matrix ceramic and polycrystalline ceramic. According to the color maps of the Y-axis a tendency of rotation occurred along X-Axis (Figure 3) because right-hand side is remarkably in tension and the left-hand side is in compression, due to experimental setting and occlusal surface geometry.

Regarding the cement variable, small differences were found in all models when comparing light-curable composite and dual-curing resin cement. However, most differences are quantitatively negligible and dependent from the observation point, with no clear pattern. Nonetheless, it is worth to notice that higher variations (high compression in the Z-axis) were found when comparing between each other the two models with resin-matrix ceramic as occlusal material (Model E and F).

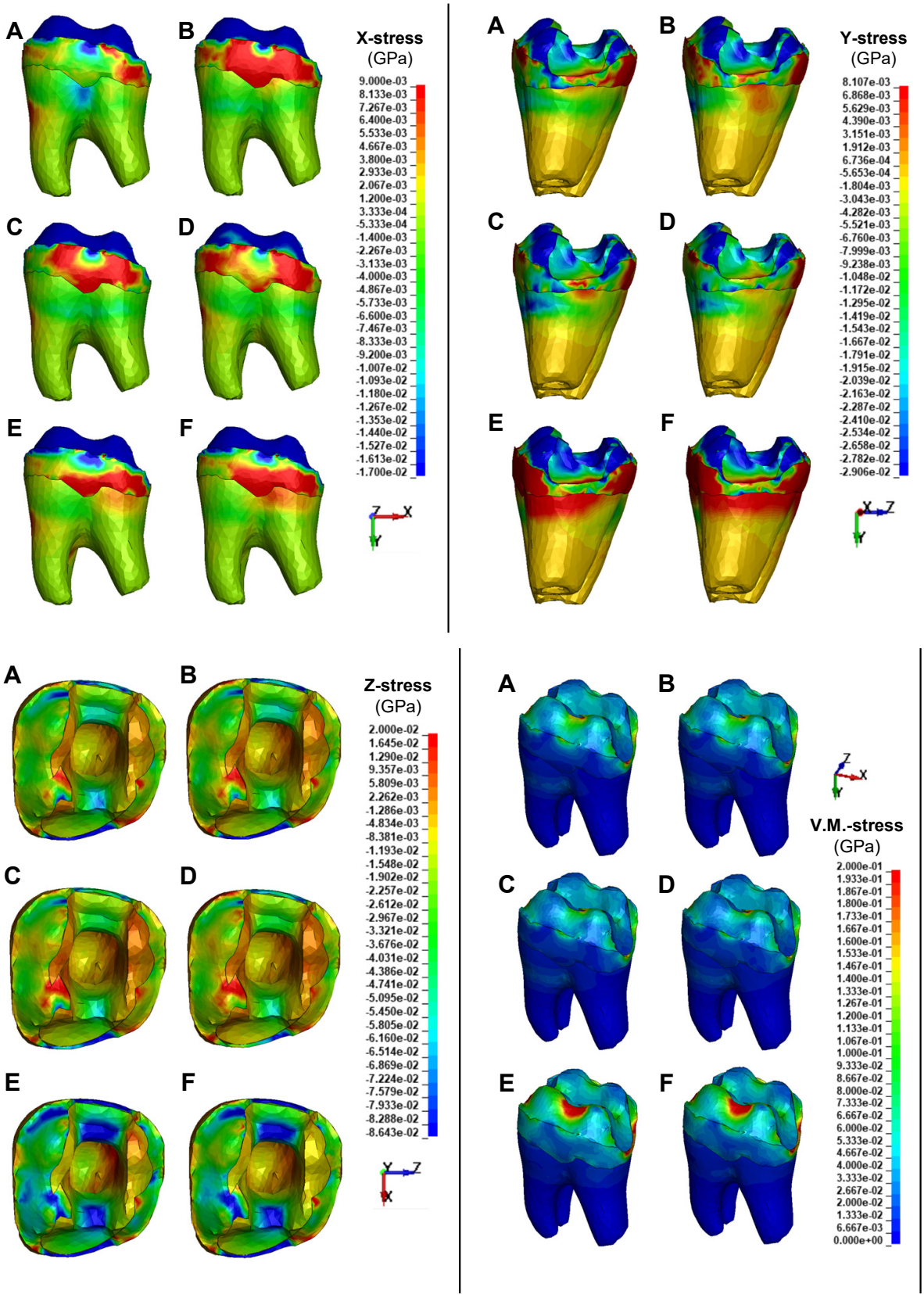


Figure 3. Resulting stresses in the different axes and Von Mises stresses of the six tested models. A dedicated color scale, expressed in GPa is reported for each axis.

3.2 Cement-restoration interface

Figure 4-6 and 7-9 report vector plot and color map respectively for normal pressure and shear stress analyses in the cement-restoration interface, in the cement restoration and in

the dentin. There is a correlation between the stress pattern and the adopted restorative material, with resin-matrix ceramic showing a wider stressed area. Stress peaks in case of normal pressure (Fig. 4-6), are located in the most coronal aspects of the interface, closer to the loading point and exactly in the spots with more residual tensions after shrinkage stress simulation. Lower stresses in the dentin are obtained using the resin-matrix cercamic (e and F) whereas these solutions present some peak in the dentin respect to the use of other material combinations. As a matter of shear stresses (Fig. 7-9), the same points are involved, but the higher stresses are concentrated in the peripheral area as well due to restoration flexion, with resin-matrix ceramic showing wider and higher stresses. The higher stresses are obtained both in dentin and restoration using the resin-matrix ceramic. The vectors stress distribution describes the interaction between the different parts of the model towards the lower direction, considering the load direction and experimental set-up.

Concerning the cement variable, small differences were found both in terms of pattern and intensity, especially when applied under the resin-matrix ceramic (Models E vs F).

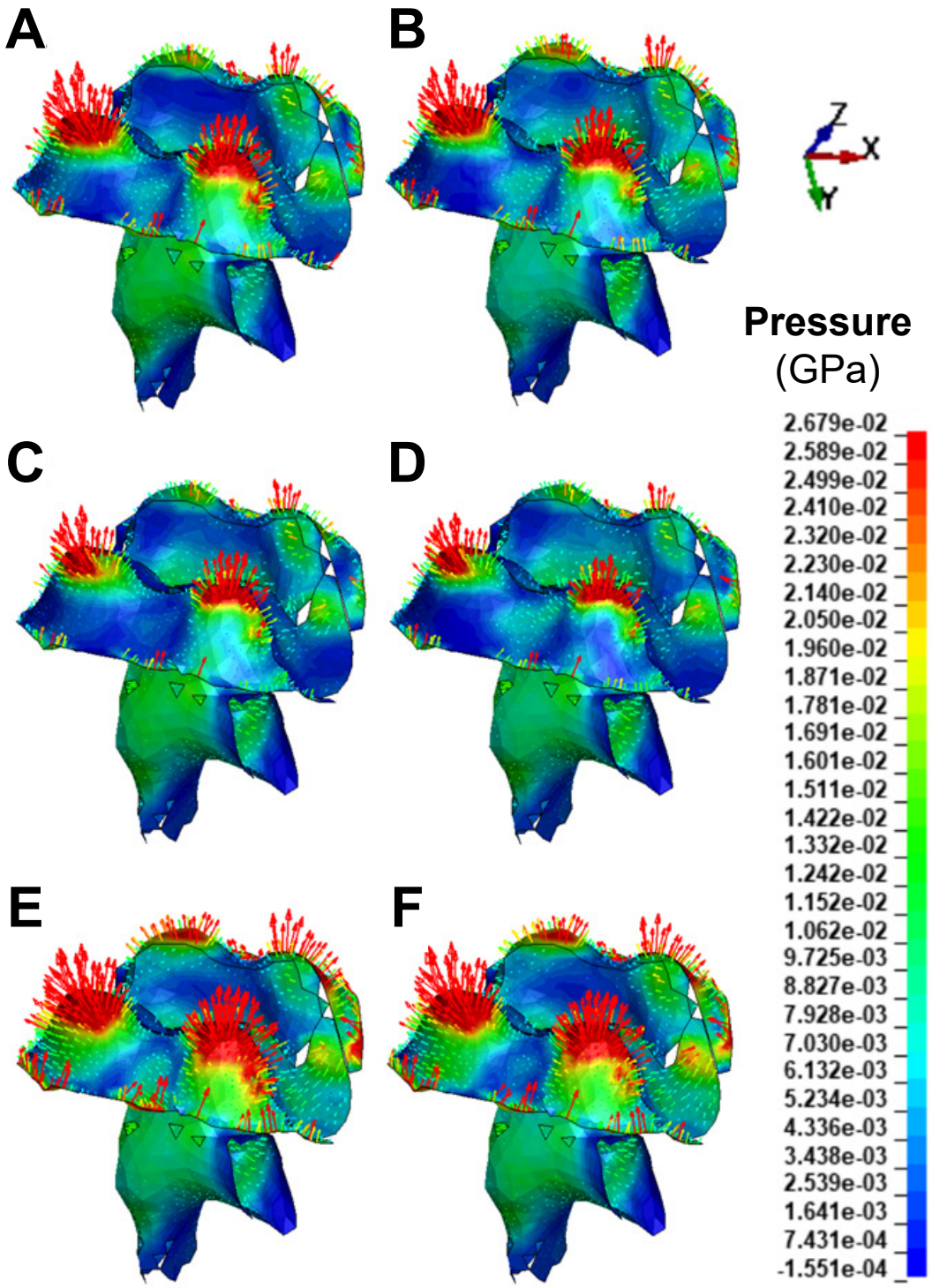


Figure 4. Vector plot of pressure distribution in cement-restoration interface of the six tested models.

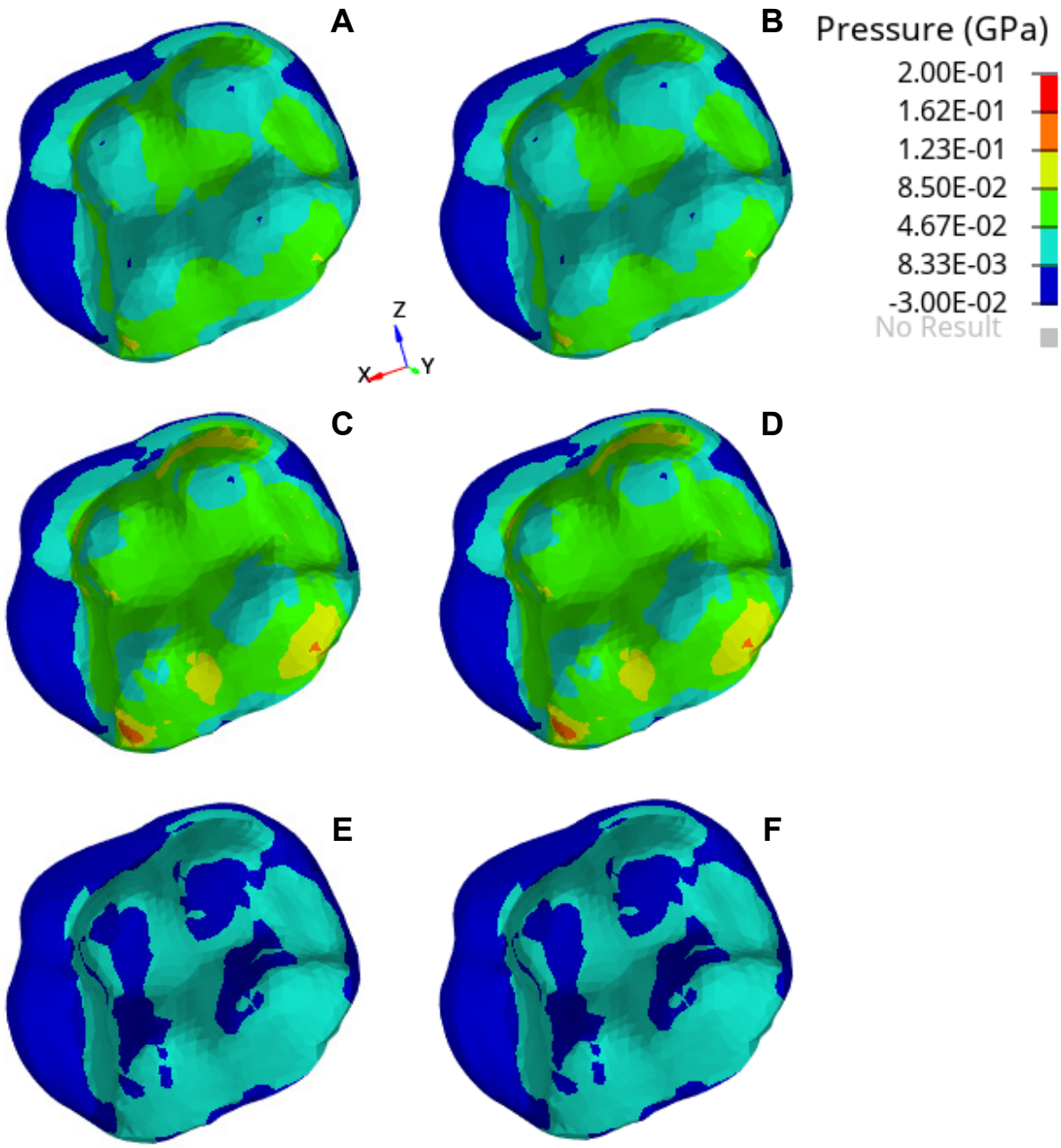


Figure 5. Pressure distribution in cement-restoration of the six tested models.

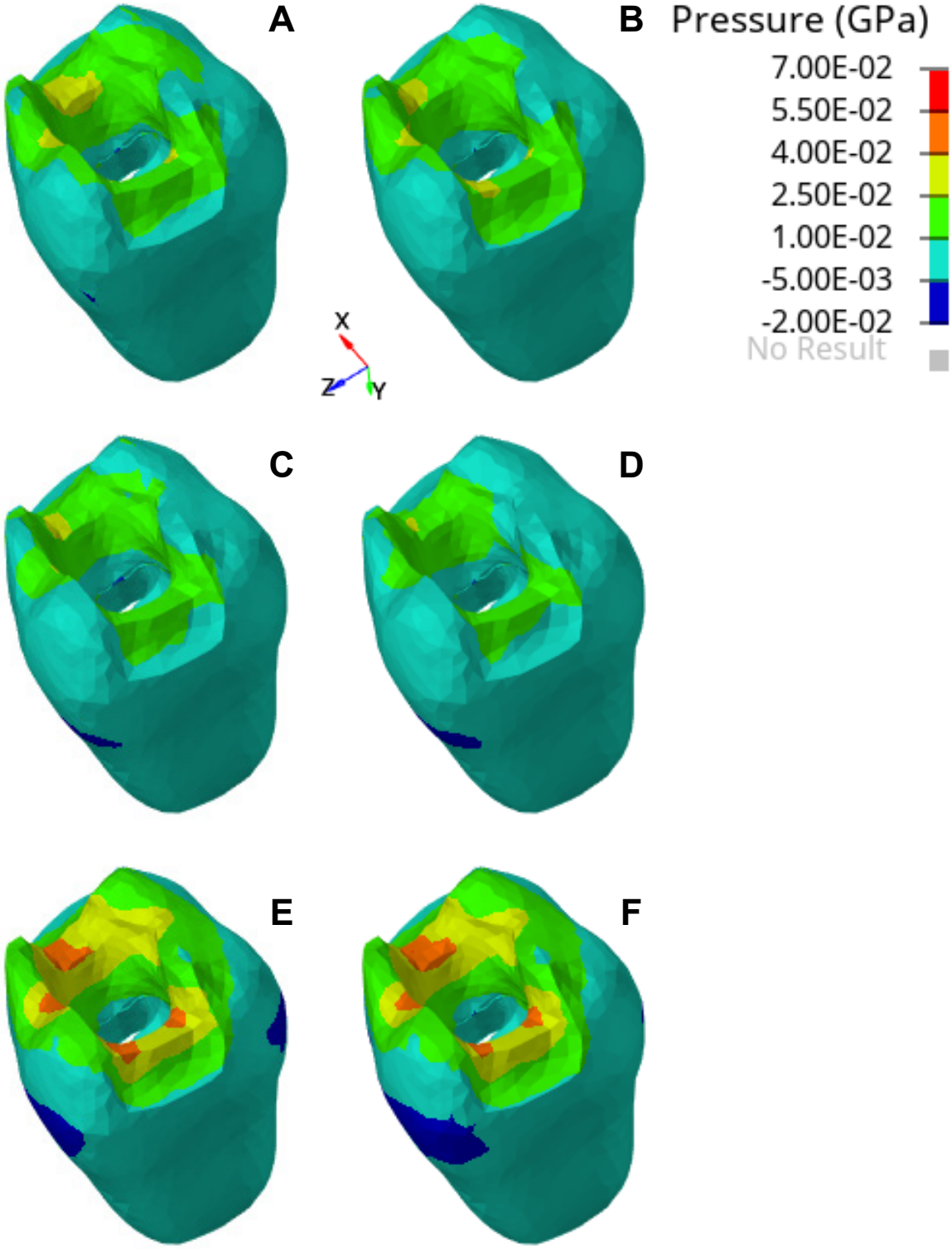


Figure 6. Pressure distribution in dentin of the six tested models.

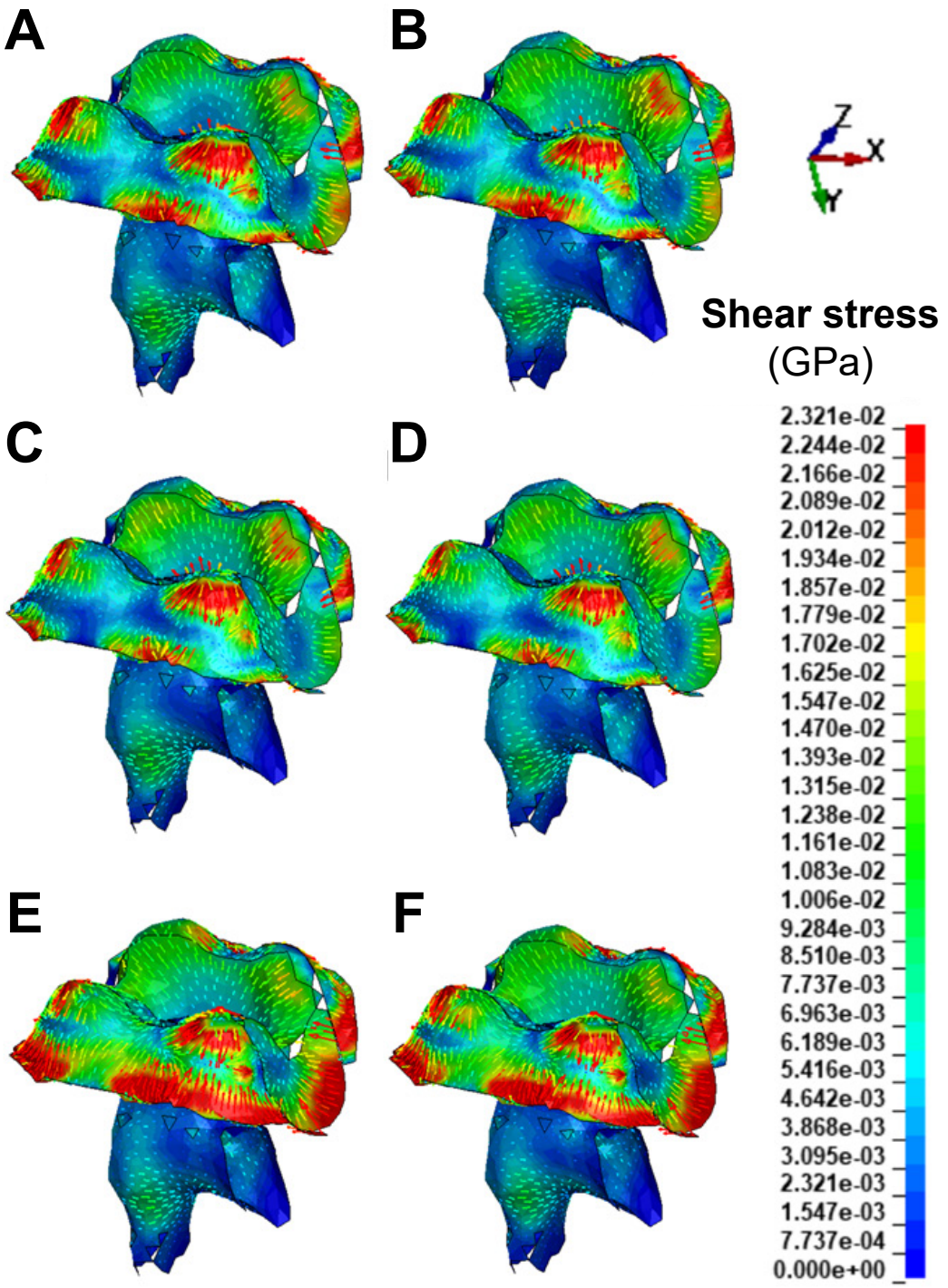


Figure 7. Vector plot of shear stresses in cement-restoration interface of the six tested models.

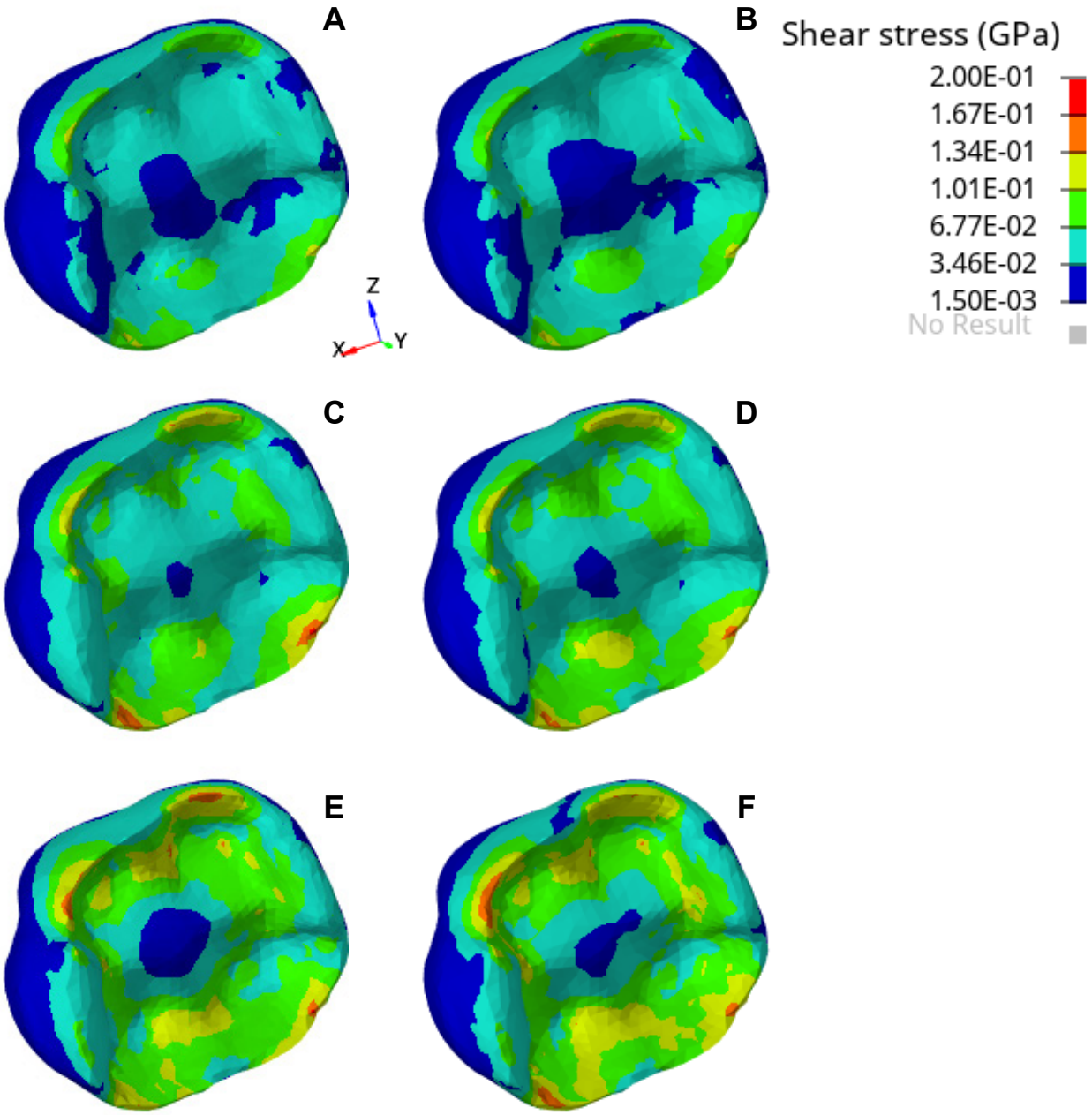


Figure 8. Shear stress distribution in cement-restoration of the six tested models.

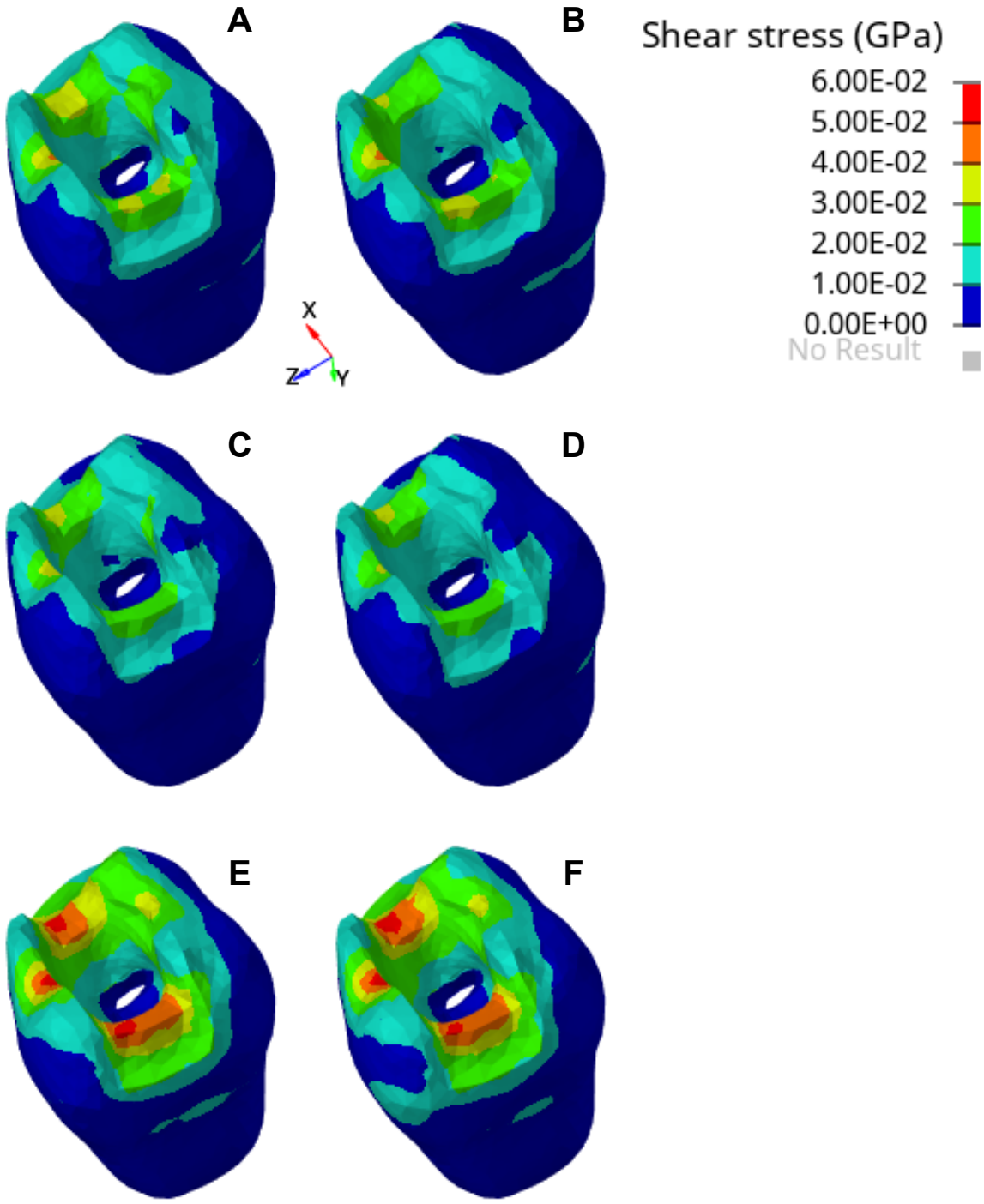


Figure 9. Shear stress distribution in dentin of the six tested models.

4. DISCUSSION

The present study analyzed with FEM the interfacial mechanical behavior of six different cement-material combinations in an indirect adhesive restoration scenario generated from micro-CT.

The protocol that was applied, from sample creation to data analysis, has already been proved to be an efficient and predictable method to evaluate the behavior of dental materials and has the massive advantage of bypassing prototyping and standardize the substrate

morphology [31]. In fact, conventionally testing on extracted teeth six different combinations would require a high sample size to achieve proper power analysis, even without considering important anatomical variables of natural teeth. Analogously to other papers, in the present study authors aimed to reproduce a clinical scenario at best creating the restoration ex-vivo and then segmenting all volumes, avoiding parts creation with CAD [32]. Even if this process is more time-consuming, real restorations will never have perfect CAD shapes and might even present defects and/or geometry limitations that have an impact on stress distribution. For the same reason, loading was not applied directly in a single central point along z-axis, but rather with a tripod-contact, which happens both in vivo and during conventional in-vitro tests. This simple shrewdness allows to have a load application and distribution which is by far more realistic, also having direct implications in the results, as will soon be discussed.

As regards the first null hypothesis, significant differences were reported between tested occlusal materials both at tooth-cement and cement-restoration interfaces. Thus, this hypothesis was rejected. In particular, model E and F (resin-matrix ceramic), showed overall higher interfacial stress peaks compared to ceramic materials. These findings were unexpected, due to the common knowledge that elastic materials express a better load distribution on the substrate, as it happens both in other direct and indirect clinical cases [34],[35],[36]. However, an explanation was found analyzing the shear vector orientation and considering the correlation of the Young's modulus with the flexibility of tested materials in the specific experimental setting (Fig. 4-9) [37]. In fact, ceramics stiffer behavior caused negligible deformation of the occlusal restoration at given load and, consequently, the load was directly transmitted on the substrate, causing stress peaks next to the loading points, specifically in the nearest point in projection [38],[31],[39]. These results are nearly identical to the ones reported in literature for crown designs, especially when considering tensile stresses and thus are not surprising [40], [41]. On contrary, resin-matrix ceramics behave the opposite due to the lower Young's modulus and thus higher flexibility at given load [42]. As aforementioned, in current experimental settings the load was not just along z-axis like other FEM studies, but rather applied in a more realistic tripod contact. This caused a tendency of rotation on the system and, consequently, the elastic restorations underwent a flexion along the bucco-lingual plane, which translates into tensile stress peaks in the cuspal area (Fig. 3). This is also confirmed by the shear stress peaks noticeable in the border area (Fig. 4,7), in which the rotation even caused an involvement of the margin. This is an important aspect that most papers in literature are not considering, often applying the load perpendicularly or with an interposed food bolus that leads to nearly the same result [43]. In authors opinion, this might underestimate the effects of shear forces that are always present during functions (especially bruxism) and have an important effect on stress

distribution [44]. It is also worth to point out that this aspect has been likely highlighted in the present setting due to the reduced presence of axial walls of the restoration in the buccal and lingual regions (e.g. conventional crown design). Indeed, axial walls have been proved to have an impact not only on the retention, but also on the stability of the system, because a wider axial area acts as stress breaker [45]. Thus, having two boxes in the mesial and distal parts probably stabilized the restoration in this direction, enhancing the rotation along the bucco-oral direction. A further crucial factor that surely emphasized this aspect is the occlusal thickness of the restoration, which was set to 1.5mm for all models. A higher occlusal thickness, at given load could reduce the flexion of the restoration, bringing to different results especially in the resin-matrix ceramic group which has the lowest Young's modulus [46]. However, giving the same thickness and occlusal morphology for all materials was essential to compare their behavior among each other. Accordingly, zirconia, which is the most rigid material tested, showed better stress distribution in the cement-tooth interface (Fig. 6,9).

Concerning the second null hypothesis, most differences among the two tested cements were quantitatively negligible and dependent from the observation point. Thus, the second null hypothesis was accepted. However, it is worth to mention that cement variable might have more importance when the occlusal material is a resin-matrix ceramic (Models E vs F). This observation is in agreement with a recent paper by Satrio Wicaksono *et al.*, that tested the influence of cement on endocrown and onlay, reporting a significant stress reduction when using light-cure resin composite compared to dual-cure resin cement [47]. This is a consequence of the higher contraction of the dual-curing resin cement, in the present study 5% vs 1.9%, which causes stress peaks in model E before loading. Even if this is not directly correlated to bond-strength degradation over time, residual stresses are essential in the subsequent development of stresses during load. Moreover, since authors purposely selected cements with similar Young's modulus, which is known to have an influence on stress distribution the differences are probably related exclusively to shrinkage simulation [48]. Thus, the fact that most differences in models A-D are negligible is in accordance with other papers in literature, which report cement thickness as a key variable rather than cement type [48],[49]. Cement thickness could also have influenced the stress distribution. In the present study, simulation was performed with a cement thickness of 80 μm in the internal area and 10 μm in the 1mm-wide marginal area, but further studies could benefit from varying such parameters and evaluate the so-obtained results [49].

A limitation of the models adopted in this paper was that the materials were simulated with homogeneous and isotropic law, despite dentin and enamel having an anisotropic behavior. However, the majority of other studies applies the same FEM protocol, due to the fact that

anisotropy can be observed only in a microscopic scale. Moreover, further efforts could be invested in the future to properly model the adhesive layer that is, in reality, positioned both on the restoration and the tooth prior cementation. However, in the present study several variables were taken into account and adding an additional artificial interface was avoided to reduce biases and misunderstandings.

The present paper is the first part of a larger FE study, that will also evaluate the effects of sliding movements on the restoration surface and it's progressive wear on interfacial stresses distribution.

5. CONCLUSION

Within the limitations of the present study, and considering that all obtained results derived from a numerical simulation, it can be concluded that:

- Load setup plays an important role in restoration flexion and thus stress behavior. Loading can be applied with a tripod contact reproducing common in-vivo scenario rather than simplified axial load.
- Resin-Matrix Ceramic models showed higher stresses in both interfaces, due to the flexion of the restoration at given load. It is likely that the absence of axial walls in the vestibular and buccal aspect, as well as the reduced occlusal thickness of the restoration enhanced this phenomenon.
- Cement type seems to have an influence only when undergoing resin-matrix ceramics, better performing when having a reduced polymerization shrinkage.

Further studies, both in-vitro and in-vivo are needed to confirm the present study results.

REFERENCES

[1] MacInnes A, Hall AF. Indications for Cuspal Coverage. Dent Update 2016;43:150–1, 154–6, 158. https://doi.org/10.12968/denu.2016.43.2.150.

[2] Rocca GT, Krejci I. Crown and post-free adhesive restorations for endodontically treated posterior teeth: from direct composite to endocrowns. Eur J Esthet Dent Off J Eur Acad Esthet Dent 2013;8:156–79.

[3] Re D, Fichera G, Devoto W. Cavity configurations for in direct partial coverage adhesive-cemented restorations. Quintessence Dent Technol 2006;29.

[4] Scotti N, Scansetti M, Rota R, Pera F, Pasqualini D, Berutti E. The effect of the post length and cusp coverage on the cycling and static load of endodontically treated maxillary premolars. Clin Oral Investig 2011;15:923–9. https://doi.org/10.1007/s00784-010-0466-y.

[5] Kishen A. Mechanisms and risk factors for fracture predilection in endodontically treated teeth 2006. https://doi.org/10.1111/J.1601-1546.2006.00201.X.

[6] Gher ME, Dunlap RM, Anderson MH, Kuhl LV. Clinical survey of fractured teeth. J Am Dent Assoc 1939 1987;114:174–7. https://doi.org/10.14219/jada.archive.1987.0006.

[7] Axelsson P, Nyström B, Lindhe J. The long-term effect of a plaque control program on tooth mortality, caries and periodontal disease in adults. Results after 30 years of maintenance. J Clin Periodontol 2004;31:749–57. https://doi.org/10.1111/j.1600-051X.2004.00563.x.

[8] Abduo J, Sambrook RJ. Longevity of ceramic onlays: A systematic review. J Esthet Restor Dent 2018;30:193–215. https://doi.org/10.1111/jerd.12384.

[9] D'Arcangelo C, Vanini L, Casinelli M, Frascaria M, De Angelis F, Vadini M, et al. Adhesive Cementation of Indirect Composite Inlays and Onlays: A Literature Review. Compend Contin Educ Dent Jamesburg NJ 1995 2015;36:570–7; quiz 578.

[10] Gracis S, Thompson V, Ferencz J, Silva N, Bonfante E. A New Classification System for All-Ceramic and Ceramic-like Restorative Materials. Int J Prosthodont 2016;28:227–35. https://doi.org/10.11607/ijp.4244.

[11] Ruse ND, Sadoun MJ. Resin-composite Blocks for Dental CAD/CAM Applications. J Dent Res 2014;93:1232–4. https://doi.org/10.1177/0022034514553976.

[12] Sulaiman TA. Materials in digital dentistry-A review. J Esthet Restor Dent. 2020 Mar;32(2):171-181. doi: 10.1111/jerd.12566. Epub 2020 Jan 13. PMID: 31943720.

[13] Silva LHD, Lima E, Miranda RBP, Favero SS, Lohbauer U, Cesar PF. Dental ceramics: a review of new materials and processing methods. Braz Oral Res. 2017 Aug 28;31(suppl 1):e58. doi: 10.1590/1807-3107BOR-2017.vol31.0058. PMID: 28902238.

[14] Ruse ND, Sadoun MJ. Resin-composite blocks for dental CAD/CAM applications. J Dent Res. 2014 Dec;93(12):1232-4. doi: 10.1177/0022034514553976. Epub 2014 Oct 24.

PMID: 25344335; PMCID: PMC4462808.

[15] D'Arcangelo C, Vanini L, Casinelli M, Frascaria M, De Angelis F, Vadini M, et al. Adhesive Cementation of Indirect Composite Inlays and Onlays: A Literature Review. Compend Contin Educ Dent Jamesburg NJ 1995 2015;36:570–7; quiz 578.

[16] Masarwa N, Mohamed A, Abou-Rabii I, Abu Zaghlan R, Steier L. Longevity of Self-etch Dentin Bonding Adhesives Compared to Etch-and-rinse Dentin Bonding Adhesives: A Systematic Review. J Evid-Based Dent Pract 2016;16:96–106. https://doi.org/10.1016/j.jebdp.2016.03.003.

[17] Rosa WL de O da, Piva E, Silva AF da. Bond strength of universal adhesives: A systematic review and meta-analysis. J Dent 2015;43:765–76. https://doi.org/10.1016/j.jdent.2015.04.003.

[18] de Assis C, Lemos C, Gomes J, Vasconcelos B, Moraes S, Braz R, et al. Clinical Efficiency of Self-etching One-Step and Two-Step Adhesives in NCCL: A Systematic Review and Meta-analysis. Oper Dent 2020;45:598–607. https://doi.org/10.2341/19-185-L.

[19] Ghodsi S, Shekarian M, Aghamohseni MM, Rasaeipour S, Arzani S. Resin cement selection for different types of fixed partial coverage restorations: A narrative systematic review. Clin Exp Dent Res. 2023 Dec;9(6):1096-1111. doi: 10.1002/cre2.761. Epub 2023 Jul 10. PMID: 37427500; PMCID: PMC10728549.

[20] Nakajima M, Arimoto A, Prasansuttiporn T, Thanatvarakorn O, Foxton RM, Tagami J. Light transmission characteristics of dentine and resin composites with different thickness. J Dent 2012;40 Suppl 2:e77-82. https://doi.org/10.1016/j.jdent.2012.08.016.

[21] Inokoshi M, Pongprueksa P, De Munck J, Zhang F, Vanmeensel K, Minakuchi S, et al. Influence of Light Irradiation Through Zirconia on the Degree of Conversion of Composite Cements. J Adhes Dent 2016;18:161–71. https://doi.org/10.3290/j.jad.a35842.

[22] Meereis CTW, Münchow EA, de Oliveira da Rosa WL, da Silva AF, Piva E. Polymerization shrinkage stress of resin-based dental materials: A systematic review and meta-analyses of composition strategies. J Mech Behav Biomed Mater. 2018 Jun;82:268-281. doi: 10.1016/j.jmbbm.2018.03.019. Epub 2018 Mar 23. PMID: 29627738

[23] Burrer P, Par M, Fürer L, Stübi M, Marovic D, Tarle Z, Attin T, Tauböck TT. Effect of polymerization mode on shrinkage kinetics and degree of conversion of dual-curing bulk-fill resin composites. Clin Oral Investig. 2023 Jun;27(6):3169-3180. doi: 10.1007/s00784-023-04928-0. Epub 2023 Mar 4. PMID: 36869923; PMCID: PMC10264464.

[24] Martorelli M, Ausiello P. A novel approach for a complete 3D tooth reconstruction using only 3D crown data. Int J Interact Des Manuf IJIDeM 2013;7:125–33. https://doi.org/10.1007/s12008-012-0166-8.

[25] Magne P. Efficient 3D finite element analysis of dental restorative procedures using micro-CT data. Dent Mater Off Publ Acad Dent Mater 2007;23:539–48. https://doi.org/10.1016/j.dental.2006.03.013.

[26] Versluis A, Tantbirojn D, Pintado MR, DeLong R, Douglas WH. Residual shrinkage stress distributions in molars after composite restoration. Dent Mater Off Publ Acad Dent Mater 2004;20:554–64. https://doi.org/10.1016/j.dental.2003.05.007.

[27] Davidson CL, de Gee AJ. Relaxation of polymerization contraction stresses by flow in dental composites. J Dent Res 1984;63:146–8. https://doi.org/10.1177/00220345840630021001.

[28] Sorrentino R, Aversa R, Ferro V, Auriemma T, Zarone F, Ferrari M, Apicella A. Three-dimensional finite element analysis of strain and stress distributions in endodontically treated maxillary central incisors restored with different post, core and crown materials. Dent Mater. 2007 Aug;23(8):983-93. doi: 10.1016/j.dental.2006.08.006. Epub 2006 Oct 30. PMID: 17070903.

[29] Baldi A, Scattina A, Ferrero G, Comba A, Alovisi M, Pasqualini D, Peroni L, Muggeo M, Germanetti F, Scotti N. Highly-filled flowable composite in deep margin elevation: FEA study obtained from a microCT real model. Dent Mater. 2022 Apr;38(4):e94-e107. Doi: 10.1016/j.dental.2021.10.005. Epub 2022 Feb 24. PMID: 35219524.

[30] Uppalapati V, Kumar S, Aggarwal R, Bhat I, Munaganti J, Khan S. Three-dimensional Finite Element Stress Pattern Analysis in Bone around Implant-supported Abutment with Different Angulations under Axial and Oblique Load. J Contemp Dent Pract. 2023 Jan 1;24(1):16-20. doi: 10.5005/jp-journals-10024-3464. PMID: 37189007.

[31] Ausiello P, Franciosa P, Martorelli M, Watts DC. Numerical fatigue 3D-FE modeling of indirect composite-restored posterior teeth. Dent Mater Off Publ Acad Dent Mater 2011;27:423–30. https://doi.org/10.1016/j.dental.2010.12.001.

[32] Verdonschot N, Fennis WM, Kuijs RH, Stolk J, Kreulen CM, Creugers NH. Generation of 3-D finite element models of restored human teeth using micro-CT techniques. Int J Prosthodont 2001;14:310–5.

[33] Tajima K, Chen KK, Takahashi N, Noda N, Nagamatsu Y, Kakigawa H. Three-dimensional finite element modeling from CT images of tooth and its validation. Dent Mater J. 2009 Mar;28(2):219-26. doi: 10.4012/dmj.28.219. PMID: 19496403.

[34] Yu H, Feng Z, Wang L, Mihcin S, Kang J, Bai S, Zhao Y. Finite Element Study of PEEK Materials Applied in Post-Retained Restorations. Polymers (Basel). 2022 Aug 22;14(16):3422. Doi: 10.3390/polym14163422. PMID: 36015679; PMCID: PMC9412468.

[35] Anatavara S, Sitthiseripratip K, Senawongse P. Stress relieving behaviour of flowable

composite liners: A finite element analysis. Dent Mater J. 2016;35(3):369-78. doi: 10.4012/dmj.2015-204. PMID: 27251991.

[36] Dal Piva AMO, Tribst JPM, Borges ALS, Souza ROAE, Bottino MA. CAD-FEA modeling and analysis of different full crown monolithic restorations. Dent Mater. 2018 Sep;34(9):1342-1350. Doi: 10.1016/j.dental.2018.06.024. Epub 2018 Jun 20. PMID: 29934125.

[37] Lawson NC, Bansal R, Burgess JO. Wear, strength, modulus and hardness of CAD/CAM restorative materials. Dent Mater Off Publ Acad Dent Mater 2016;32:e275–83. https://doi.org/10.1016/j.dental.2016.08.222.

[38] Sulaiman TA, Suliman AA, Mohamed EA, Rodgers B, Altak A, Johnston WM. Mechanical Properties of Bisacryl-, Composite-, and Ceramic-resin Restorative Materials. Oper Dent. 2022 Jan 1;47(1):97-106. Doi: 10.2341/20-191-L. PMID: 35029680.

[39] Zhu J, Rong Q, Wang X, et al. Influence of remaining tooth structure and restorative material type on stress distribution in endodontically treated maxillary premolars: a finite element analysis. J Prosthet Dent. 2017;117:646–655. doi: 10.1016/j.prosdent.2016.08.023.

[40] Sichi LGB, Pierre FZ, Arcila LVC, de Andrade GS, Tribst JPM, Ausiello P, di Lauro AE, Borges ALS. Effect of Biologically Oriented Preparation Technique on the Stress Concentration of Endodontically Treated Upper Central Incisor Restored with Zirconia Crown: 3D-FEA. Molecules. 2021 Oct 10;26(20):6113. Doi: 10.3390/molecules26206113. PMID: 34684695; PMCID: PMC8538003.

[41] Dal Piva AMO, Tribst JPM, Borges ALS, Souza ROAE, Bottino MA. CAD-FEA modeling and analysis of different full crown monolithic restorations. Dent Mater. 2018 Sep;34(9):1342-1350. Doi: 10.1016/j.dental.2018.06.024. Epub 2018 Jun 20. PMID: 29934125.

[42] Zimmerli B, Strub M, Jeger F, Stadler O, Lussi A. Composite materials: composition, properties and clinical applications. A literature review. Schweiz Monatsschrift Zahnmed Rev Mens Suisse Odonto-Stomatol Riv Mens Svizzera Odontol E Stomatol 2010;120:972–86.).

[43] https://doi.org/10.1016/j.jmbbm.2024.106409.

[44] Ausiello P, Apicella A, Davidson CL, Rengo S. 3D-finite element analyses of cusp movements in a human upper premolar, restored with adhesive resin-based composites. J Biomech 2001;34:1269–77. https://doi.org/10.1016/s0021-9290(01)00098-7.

[45] Baldi A, Comba A, Ferrero G, Italia E, Michelotto Tempesta R, Paolone G, Mazzoni A, Breschi L, Scotti N. External gap progression after cyclic fatigue of adhesive overlays and crowns made with high translucency zirconia or lithium silicate. J Esthet Restor Dent. 2022 Apr;34(3):557-564. Doi: 10.1111/jerd.12837. Epub 2021 Nov 16. PMID: 34783440; PMCID:

PMC9298883.

[46] Tribst JPM, Dal Piva AMO, Penteado MM, Borges ALS, Bottino MA. Influence of ceramic material, thickness of restoration and cement layer on stress distribution of occlusal veneers. Braz Oral Res. 2018 Nov 29;32:e118. doi: 10.1590/1807-3107bor-2018.vol32.0118. PMID: 30517427.

[47] Wicaksono S, Prasetia W, Muryani A, Dirgantara T, Mahyuddin AI. Finite element stress analysis of dental cement application on endocrown and onlay restoration. Aust Endod J. 2023 Dec;49(3):665-674. doi: 10.1111/aej.12800. Epub 2023 Oct 3. PMID: 37789568.

[48] He J, Zheng Z, Wu M, Zheng C, Zeng Y, Yan W. Influence of restorative material and cement on the stress distribution of endocrowns: 3D finite element analysis. BMC Oral Health. 2021 Oct 5;21(1):495. doi: 10.1186/s12903-021-01865-w. PMID: 34610825; PMCID: PMC8491409.).

[49] Mounica Y, Behera S, Arunachalam S, Srikanth L, Deepthi MN, Susmita M. Influence of Different Cements and Cement Thickness on the Stress Distribution under Occlusal Surfaces of Porcelain-fused-to-metal and Porcelain-fused-to-zirconium Crowns: A Finite Element Analysis. J Contemp Dent Pract. 2022 Dec 1;23(12):1224-1229. doi: 10.5005/jp-journals-10024-3448. PMID: 37125520.